Rate-Limiting Steps in Oxidations Catalyzed by Rabbit Cytochrome P450 1A2[†]

F. Peter Guengerich,* Joel A. Krauser, and William W. Johnson[‡]

Department of Biochemistry and Center in Molecular Toxicology, Vanderbilt University School of Medicine, Nashville, Tennessee 37232-0146

Received April 28, 2004; Revised Manuscript Received June 24, 2004

ABSTRACT: Several issues regarding the rate-limiting nature of individual reaction steps in catalysis by rabbit liver cytochrome P450 (P450) 1A2 were addressed using anisoles and other substrates. Substrate binding is very fast ($k > 10^6$ M^{-1} s^{-1}). Product release is not rate-limiting, as shown by the absence of bursts, placing rate-limiting steps at or before product formation. We had previously shown that the first 1-electron reduction step is fast ($k > 700$ min^{-1}), even in the absence of ligand [Guengerich, F. P., and Johnson, W. W. (1997) *Biochemistry 36*, 14741−147500]. O_2 binding to ferrous P450 is fast ($k \geq 10^6$ M^{-1} s^{-1}). The decay of the P450 Fe^{2+}−substrate−O_2 complex was slow in the absence of NADPH−P450 reductase, with a first-order rate constant of 14 min^{-1} at 25 °C. During the decay, product was formed (from the substrate methacetin) in 61% theoretical yield, although this reaction requires electron transfer among P450 molecules and may not be related to normal turnover. Steady-state spectra suggest that one or more iron−oxygen complexes accumulate, representing entities between the Fe^{2+}−O_2 complex and putative FeO^{3+} entity. Kinetic isotope effect experiments were done with several substrates, mainly anisoles. Apparent intrinsic deuterium isotope effects as high as 15 were measured. In all cases, the C−H bond-breaking step is at least partially rate-limiting. The isotope effects were not strongly attenuated in noncompetitive or competitive experiments, consistent with relatively rapid P450−substrate exchange, except with the active enzyme Fe−O complex. Kinetic simulations with the available data (i) are consistent with the view that C−H bond breaking is a major rate-limiting step, (ii) demonstrate that increasing the rate of this step will affect k_{cat}, K_m, and kinetic hydrogen isotope effects but will only increase catalytic efficiency to a certain degree, (iii) indicate that increasing ground-state binding can increase catalytic efficiency but not k_{cat}, and (iv) suggest that nonproductive binding modes and abortive reduction of O_2 are factors that attenuate catalytic efficiency.

Cytochrome P450 enzymes are of widespread interest because of their presence in organisms ranging from Archebacters to humans (*4*). The mammalian enzymes are of particular medical relevance because of their important roles in the metabolism of drugs, steroids, carcinogens, and other endobiotic and xenobiotic chemicals (*4*−*6*). The variety of oxidative reactions that P450s catalyze using a general chemical mechanism is of particular interest (*7*, *8*).

The catalytic cycle for P450[1] oxidations is complex, probably involving at least nine steps independent of protein conformational changes (Scheme 1, with steps 5 and 6 both shown as composites) (*7*, *8*, *10*). The complexity of the mechanism produces uncertainty as to what observed steady-state parameters represent, e.g., k_{cat} and K_m (*10*, *11*). Efforts to identify rate-limiting steps go back to shortly after the discovery of the P450 system (*12*−*16*). These efforts have continued to this day, and different P450s and reactions follow multiple courses (*10*, *17*, *18*).

Scheme 1: General Scheme for P450 Catalysis[a]

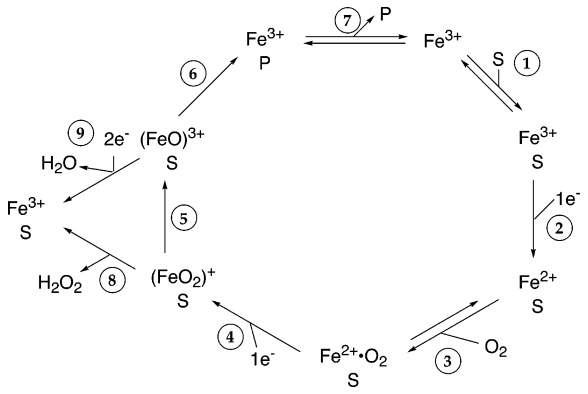

[a] Fe = iron atom of the P450 prophyrin, S = substrate, and P = product (*7*, *9*).

One approach to the analysis of rate-limiting steps is the direct measurement of potential individual steps and consideration of their rates in the context of steady-state reaction rates (*19*). Another approach is the study of the effects of isotopic substitution of substrates and the resulting effects

[†] Supported by U.S. Public Health Service Grants R01 CA90426, R35 CA44353, P30 ES00267, T32 ES07028, and F32 ES05663.

* Corresponding author. Telephone: (615) 322-2261. Fax: (615) 322-3141. E-mail: f.guengerich@vanderbilt.edu.

[‡] Present address: OSI Pharmaceuticals, 2860 Wilderness Place, Boulder, CO 80301.

[1] Abbreviations: P450, cytochrome P450 [also termed "heme−thiolate protein P450" (*1*)]; HPLC, high-performance liquid chromatography; MS, mass spectrometry; αNF, α-naphthoflavone (7,8-benzoflavone); di-12:0 GPC, L-α-dilauroyl-*sn*-glycero-3-phosphocholine. The conventions ^{D}k = intrinsic kinetic deuterium isotope effect, $^{D}V = {}^{H}k_{cat}/{}^{D}k_{cat}$, and $^{D}(V/K) = {}^{H}(k_{cat}/K_m)/{}^{D}(k_{cat}/K_m)$ of Northrop (*2*, *3*) are used in the designation of kinetic hydrogen isotope effects (H = protium; D = deuterium).

10.1021/bi0491393 CCC: $27.50
Published on Web 07/29/2004

on rates (*2*), particularly C−H bond breaking in the case of P450s. The study of kinetic hydrogen isotope effects in P450 research is >30 years old (*13*). Significant kinetic deuterium isotope effects were first reported in some reactions in crude microsomal preparations (*20*, *21*). Groves et al. (*22*) used the high isotope effect observed for norbornane hydroxylation as a tenet of the hydrogen atom abstraction/rebound mechanism for P450 catalysis. The existence of significant kinetic hydrogen isotope effects in P450 reactions is generally acknowledged; effects have even been observed in vivo (*23*−*25*). However, many of the studies in the literature were done using a variety of competitive and noncompetitive approaches, and there has been some confusion about the interpretation, particularly when the results are grouped and treated together (*15*, *26*).

Miwa and Lu considered the importance of the intrinsic kinetic deuterium isotope effect (^{D}k), which is most analogous to an isotope effect measured in a purely chemical reaction (*3*), and its attenuation by other reaction steps (*26*−*29*). Calculated intrinsic isotope effects for some reactions were as high as 14, but these were strongly attenuated (*27*). In one case (7-ethyloxycoumarin O-deethylation measured in hamster liver microsomes), the ^{D}k (5.5) was not attenuated (*29*). Other theoretical and experimental discussions of the attenuation of P450 intrinsic isotope effects followed, with a variety of microsomal P450 systems (*30*−*34*). Work with bacterial P450 101 ($P450_{cam}$) indicates that the C−H bond-breaking step is probably not rate-limiting with the preferred substrate camphor (*35*) but becomes limiting with modified, less rapidly oxidized substrates (*36*, *37*). Noncompetitive intermolecular isotope effect experiments provide the most direct information about the rate-limiting nature of the C−H bond-breaking step, although surprisingly few studies use this experimental approach in the analysis of isotope effects (*17*, *18*, *27*, *29*, *38*−*41*).

We have been interested in defining rate-limiting steps in P450 reactions (*8*, *10*). The reasons why the mammalian P450s are generally much slower than many of those catalyzed by bacterial P450s are still unclear (*42*). Further, a better understanding of why particular steps are slow could be utilized in efforts to improve P450s through mutagenesis for practical purposes (*43*, *44*). We have analyzed some aspects of the rate-limiting nature of human P450 1A2 in this regard (*40*, *41*, *43*). Rabbit P450 1A2 has somewhat different properties than human P450 1A2 (*45*) and has been the subject of numerous mechanistic investigations (*46*−*50*).

We present an extended study of aspects of kinetic analysis of individual reaction steps, using a variety of approaches including pre-steady-state kinetics and kinetic deuterium isotope effects. We conclude that the rate of C−H bond breaking is a major limitation, at least with the reactions under consideration. Some very high ^{D}k effects (∼15) were fully expressed. Kinetic modeling of individual rate constants and discussion of their potential rate-limiting natures are also presented.

EXPERIMENTAL PROCEDURES

Chemicals. Unless stated otherwise, most chemicals were obtained from Aldrich Chemical Co. (Milwaukee, WI). Methacetin (4-methoxyacetanilide) was purchased from Acros Organics (Geel, Belgium). Anisoles were recrystallized (C_2H_5OH/H_2O) before use. CD_3I (99.5% atomic excess), CD_2HI (99% atomic excess), $^{13}CH_3I$, and $^{13}CD_3I$ were purchased from Cambridge Isotopes (Cambridge, MA) or Aldrich.

The general approach to preparation of methyl-labeled anisoles involved heating the appropriate phenol with a 1.1-fold molar excess of both methyl iodide and K_2CO_3 in acetone (under reflux) for 40 h, followed by filtration of the K_2CO_3, concentration to dryness, washing of a CH_2Cl_2 solution three times with aqueous 10% Na_2CO_3 (w/v), drying (of the CH_2Cl_2 layer) with Na_2SO_4, concentration to dryness, and crystallization from C_2H_5OH/H_2O mixtures. Yields varied from 46% to 76%, except for the synthesis of deuterated 1,4-dimethoxybenzene from hydroquinone (17%). The following melting point data (obtained using a Mel-Temp device; Laboratory Devices, Cambridge, MA; uncorrected) were collected (all substitution on the methoxy group): 4-nitroanisole, d_2 51−52 °C, d_3 51−53 °C, $^{13}C/d_0$ 50−53 °C, $^{13}C/d_3$ 50−53 °C; 4-cyanoanisole, d_2 58−60 °C, d_3 58.5−59.5 °C, $^{13}C/d_0$ 56−59 °C, $^{13}C/d_3$ 53−56 °C; 1,4-dimethoxybenzene, d_3/d_0 54−56 °C, d_2/d_2 55−57 °C, d_6 51−53 °C; methacetin, d_3 125−127 °C, $^{13}C/d_0$ 127−130 °C, $^{13}C/d_3$ 125−128 °C. [*methoxy*-d_2]Methacetin had been prepared previously (*41*). [*acetamido*-d_3]Methacetin ($CH_3OC_6H_4NHCOCD_3$) was prepared by the reaction of 4-anisidine with $(CD_3CO)_2O$ in pyridine (*41*) (mp 127−130 °C). Structures of all samples were confirmed by ^1H NMR (in $CDCl_3$) and mass spectrometry. The isotopic content of all d_3-substituted anisoles was >98% as judged by integration of the methyl signal.

[*acetamido*-d_1]Methacetin ($CH_3OC_6H_4NHCOCH_2D$) was prepared using the following procedure. Bromoacetic acid (5 g, 36 mmol) was dissolved in dry tetrahydrofuran (50 mL) and chilled on ice. $LiB(C_2H_5)_3D$ (Super-Deuteride; Aldrich; 1 M, 100 mL) was added dropwise to the solution, which was then warmed to room temperature, heated under reflux for 2 h, and stirred overnight. The reaction was slowly quenched with a minimal amount of a 1:1 mixture of an aqueous 2 N NaOH−30% H_2O_2 solution (v/v). Tetrahydrofuran was removed in vacuo, and the solution was acidified to pH 3 with H_2SO_4. The acidified aqueous solution was extracted with $(C_2H_5)_2O$ (3 × 150 mL) [the $(C_2H_5)_2O$ had been passed through a silica column three times to remove any residual unlabeled acetic acid present], and the organic layer was dried over $MgSO_4$. $(C_2H_5)_2O$ was removed in vacuo (room temperature), and the remaining liquid was distilled at atmospheric pressure (105−112 °C). Excess H_2O was azeotroped from the distillate using a Dean−Stark trap and benzene. The dry solution was chilled on ice, and dry pyridine (1 mL) was added, followed by $SOCl_2$ (0.6 mL). The resulting benzene solution of d_1-acetyl chloride was used directly in the next step. *p*-Methoxyaniline (300 mg) was dissolved in benzene (20 mL) containing 0.6 mL of pyridine, and the resulting solution was added to a chilled solution of the above prepared d_1-acetyl chloride in benzene (25 mL). The solution was warmed to room temperature and stirred overnight. The reactions were extracted with saturated aqueous $NaHCO_3$ (2 × 50 mL) and then brine (25 mL). The benzene layers were dried with $MgSO_4$, benzene was removed under reduced pressure, and the solid was purified by chromatography on silica using a CH_2Cl_2−ethyl acetate mobile phase (3:1 v/v), concentrated to dryness from the

solvents, and crystallized (C_2H_5OH). MS indicated >99% isotopically enriched [*acetamido-d*$_1$]methacetin (40% yield).

7-Methoxyresorufin (both d_0 and d_3) was prepared by heating 7-hydroxyresorufin (Aldrich) with a 1.1-fold excess each of CH_3I (or CD_3I) and K_2CO_3 in *N*,*N*-dimethylformamide at 45 °C for 24 h (in the dark). The workup was as in the case of the labeled anisoles, except that the *N*,*N*-dimethylformamide was removed with a high vacuum pump and the product was purified by flash chromatography (silica gel) using elution with $CHCl_3-CH_3CN$ (9:1 v/v), followed by concentration in vacuo and crystallization from acetone: d_0 mp 252−253 °C, d_3 253−254 °C [cf. mp 253−254 °C (*51*)], >99% isotopic purity for d_3 as judged by the δ 3.94 ^{1}H NMR peak (in $CDCl_3$).

All substrates were prepared as CH_3CN solutions except for 7-methoxyresorufin, which was dissolved in $(CH_3)_2SO$ for use in enzymatic reactions.

Enzymes. Rabbit P450 1A2 was purified from liver microsomes isolated from 5,6-benzoflavone-treated rabbits as described previously (*52*) and modified in this laboratory (*45*). Rat P450 1A2 was purified from liver microsomes isolated from isosafrole-treated rats as described (*53*). Our experience to date with P450 1A2 enzymes (from rat, rabbit, and human) indicates that all need to be maintained in buffer with an ionic strength ≥0.1 M potassium phosphate to avoid precipitation. Rat NADPH−P450 reductase was expressed in *Escherichia coli* and purified to apparent homogeneity as described (*54*).

Enzyme Reactions (Steady State). Most of the reactions involved the reconstitution of (rabbit) P450 1A2 with a 1.5−2-fold excess of NADPH−P450 reductase in 0.10 M potassium phosphate buffer (pH 7.4) containing 45 μM di-12:0 GPC and an NADPH-generating system consisting of 0.5 mM $NADP^+$, 10 mM glucose 6-phosphate, and 1 IU of yeast glucose 6-phosphate dehydrogenase mL^{-1} (*55*). For most of the steady-state O-demethylation reactions [and conversion of methacetin or phenacetin to an acetol (*40*)], the reactions involved volumes of 0.5 mL and a P450 concentration of 0.5 μM. Substrates, dissolved in CH_3CN unless stated otherwise, were added at varying concentrations, with a CH_3CN (or other solvent) concentration of 1% (v/v). In most steady-state O-demethylation (or acetol formation) reactions the incubation time was 5 min (at 37 °C). Reactions were stopped by the addition of 43% H_3PO_4 (0.1 volume/reaction volume, e.g., 50 μL/0.5 mL reaction). Products (and substrate) were extracted with 4 volumes of CH_2Cl_2 or, in the case of methacetin or phenacetin, a 4:1 mixture of $CHCl_3$−2-propanol (v/v). After being mixed with a vortex device, the layers were separated by centrifugation [$(2 \times 10^3)g$, 10 min], and an aliquot (usually 80%, e.g., 1.6 mL of a total of 2.0 mL) was transferred to a new vial or tube and concentrated to dryness under an N_2 stream (at room temperature).

In some experiments, the conversion of 1,4-dimethoxybenzene to 4-methoxyphenol was estimated by a microcolorimetric procedure. The extracted residues were mixed with 0.20 mL of Gibb's reagent (5 mM 2,6-dichloroquinone-4-chloroimide in C_2H_5OH) (*56*) diluted 10-fold in 0.2 M sodium borate buffer (pH 9.3) prior to use. The derivatized products were extracted into 1.0 mL of 1-butanol, and the absorbance was measured at 650 nm (and compared to a series of 4-methoxyphenol standards).

Most of the O-demethylation assays involved the analysis of the resulting phenols by reversed-phase HPLC. A 6.2 mm × 80 mm Zorbax octadecylsilane (C_{18}) HPLC column (3 μm; MacMod, Chadds Ford, PA) was used with the following solvent systems: 4-nitrophenol, 27% CH_3CN (v/v) in 20 mM NH_4HCO_2 (pH 4.5), flow 3.0 mL min^{-1}, detector A_{316}; 4-cyanophenol, 27% CH_3CN (v/v) in 20 mM NH_4HCO_2 (pH 4.5), flow 3.0 mL min^{-1}, detector A_{245}; 4-hydroxyanisole, 27% CH_3CN (v/v) in 20 mM NH_4HCO_2 (pH 4.5), flow 3.0 mL min^{-1}, detector A_{288}; acetaminophen and methacetin (or phenacetin) acetol, gradient (solvent A = $H_2O/CH_3OH/CH_3CO_2H$, 95:5:0.15 v/v/v; solvent B = CH_3CN/H_2O, 9:1 v/v) consisting of 100% solvent A for $t = 0-2$ min, linear gradient to 30% solvent B from $t = 2$ to 10 min, hold at 30% solvent B from $t = 10$ to 13 min, linear gradient to 100% solvent A from $t = 13$ to 15 min, flow 3.0 mL min^{-1}, detector A_{254}.

7-Methoxyresorufin O-demethylation was measured using a continuous fluorometric assay (excitation 530 nm, emission 588 nm).

NADPH oxidation (ΔA_{340}) and H_2O_2 formation were measured as described elsewhere (*40*), and H_2O formation was estimated by the difference method (*40*, *57*).

2,4-Dinitrophenylhydrazone derivatives of formaldehyde were prepared as described (*58*) and used to estimate kinetic hydrogen isotope effects. Analysis was done either by gas chromatography/electron impact MS (positive-ion electrospray) (*40*, *58*, *59*) or by HPLC/MS. In some cases the competitive experiments were done with ^{13}C- and ^{13}C,D-labeled anisoles to reduce the artifacts associated with endogenous HCHO present in reagents.

Anaerobic Experiments. The basic system is described elsewhere (*60*, *61*). In the course of the work the gas train/manifold system was modified to delete the heated glass tower of BASF copper catalyst and replace it with two coils of Alltech Oxy-Trap catalyst (Alltech Associates, Deerfield, IL), in-line between the Ar tank and the water sparging bottle (before the manifold). The water bottle was filled with a solution of 0.50 mM safranine T, 0.67 M Tris·HCl (pH 7.7), 33 mM EDTA, and 0.2 mM methyl viologen, which acts as a redox indicator to sense O_2 contamination ($E_{m,7}$ of methyl viologen = −440 mV, with the blue color indicative of the reduced form) and can be photoreduced (with the safranine T).

For anaerobic stopped-flow experiments, the instrument drive syringes were flushed with anaerobic buffer, filled with a solution of safranine T in Tris−EDTA buffer (vide supra), and illuminated (with a lamp) to scrub the system (with N_2 flowing through the bath outside the syringes). The dye solution was flushed with anaerobic buffer, and then anaerobic samples were introduced from tonometers.

Spectroscopy. UV−visible spectra were collected on either an OLIS-Aminco DW-2a or an OLIS-Cary 14 instrument (OLIS, Bogart, GA) or, in the case of stopped-flow experiments, with an Applied Photophysics SX-17 MV (Applied Photophysics, Leatherhead, U.K.) or an OLIS RSM-1000 instrument.

Kinetic Deuterium Isotope Effects. Several types of experiments were used, and the results provide different information about the relative rates of different events (Scheme 2). In *intermolecular noncompetitive* experiments (Scheme 2A), separate sets of steady-state assays of product formation were

Scheme 2: Kinetic Hydrogen (Deuterium) Isotope Experiments[a]

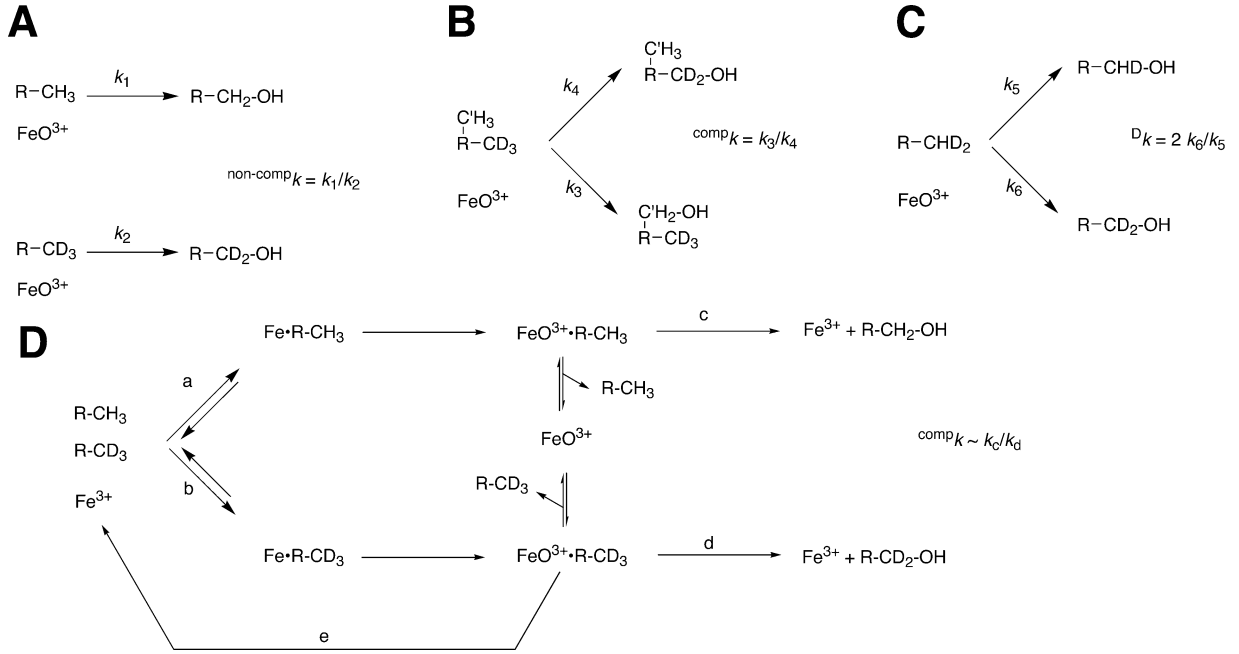

[a] RCH_3, $C'H_3$ denotes a substrate with two potential sites of oxidation (shown as methyl groups in this example) in parts A−C, with $-CH_3$ as the preferred site of hydroxylation. (A) Noncompetitive intermolecular experiment; (B) competitive intramolecular experiment; (C) "noncompetitive" intramolecular experiment (estimate of intrinsic deuterium kinetic isotope effect, most relevant in the case of a methyl group); (D) competitive intermolecular experiment. See text for further discussion.

done with a single enzyme preparation, one set using d_0 substrate and the other using d_3-methoxy substrate. In both cases the substrate concentration was varied (usually 14 concentrations each for d_0 and d_3, with duplicate assays for each concentration) (d_6 substrate was used in the case of 1,4-dimethoxybenzene). The results were fit to hyperbolic plots of v vs S using nonlinear regression analysis (Graphpad Prism; Graphpad, San Diego, CA), with SE calculated. The results are expressed as either ${}^{D}V = {}^{H}k_{cat}/{}^{D}k_{cat}$ or ${}^{D}(V/K) = ({}^{H}k_{cat}/{}^{H}K_m)/({}^{D}k_{cat}/{}^{D}K_m)$, using the convention of Northrop (*2*, *3*).[1] These experiments provide a measure of the contribution of the C−H bond-breaking step to limiting the reaction rate.

Intramolecular competitive experiments (Scheme 2B) were done with 1,4-dimethoxybenzene. In this situation the two methoxy groups are equivalent, and only one was labeled ($CD_3O-C_6H_4-OCH_3$). Incubations were run with a single substrate concentration (100 μM), and the deuterium content of the product $CD_3OC_6H_4OH/CH_3OC_6H_4OH$ was determined using HPLC/MS and the ratio of the ions (MH^+) m/z 128/125 = ${}^{D}(V/K)$, by definition (*3*).

Intramolecular noncompetitive experiments involved the oxidation of d_2-methyl groups (CD_2H-) (Scheme 2C). Because of the rapid rotation of methyl groups, prochirality is not an issue. The product formaldehyde was recovered as the 2,4-dinitrophenylhydrazone and analyzed by gas chromatography/MS. The ratio of the peaks (M^+) at m/z 212 and 211, multiplied by 2 (and corrected for ^{13}C contributions), gives the isotope effect, which is regarded as an estimate of ${}^{D}k$, the intrinsic isotope effect. In the case of [*acetyl-d*$_2$]-methacetin, the acetol product was assayed directly using on-line HPLC/MS (electrospray positive ion mode), and ${}^{D}k$ = ratio of peaks at m/z 182:183 after correction for ^{13}C.

Intermolecular competitive experiments involved a 1:1 mixture of d_0 substrate and perdeuterated substrate (Scheme 2D). Analysis of the product formaldehyde as the 2,4-dinitrophenylhydrazone (gas chromatography/MS) gives the ratio of the intensities of the m/z 210 and 212 ions, which is the ${}^{D}(V/K)$ in this experiment (*3*). In one experiment, the rates of oxidation of varying concentrations of the substrates d_0-4-cyanoanisole, d_3-4-cyanoanisole, and a 1:1 mixture of d_0 and d_3 4-cyanoanisole were compared (analysis of 4-cyanophenol by HPLC/UV measurements). A similar approach was used with methacetin for acetol measurement [HPLC/MS, with comparison of intensities at m/z 182 and 184 (MH^+)].

Limited Cycle Experiments. In each case the electron input was limited to allow the P450 1A2 to only proceed through a single cycle, plus the use of electrons from the reduced accessory protein (reductase) or dye. P450 1A2 (45 nmol in 3.0 mL of 0.10 M potassium phosphate buffer, pH 7.4, containing 68 μM di-12:0 GPC and 500 μM methacetin) was supplemented with either (i) 45 nmol of NADPH−P450 reductase or (ii) a mixture of 0.10 M Tris·HCl (pH 7.4), 10 mM EDTA, 5 μM 5-deazaflavin, and 1 μM safranine T. One of the part i reactions was mixed with 135 nmol of NADPH (90 nmol for the reductase, which contains 1 FAD and 1 FMN) in the presence of air, and the reaction was quenched with 0.30 mL of 43% H_3PO_4. The other part i mixture was deaerated in an anaerobic cuvette, and 135 nmol of NADPH was tipped into the main compartment from a side arm. Reduction was monitored in a spectrophotometer. The sample was then opened and mixed with air. The reaction was quenched with 0.30 mL of 43% H_3PO_4. The part ii sample was deaerated and reduced photochemically (visible light source, 500 W, ~3 min) with the reaction monitored using a spectrophotometer. The reduction of the indicator dye safranine T was also noted. The sample was opened and mixed with air. The reaction was quenched with 0.30 mL of 43% H_3PO_4. The methacetin products were extracted and

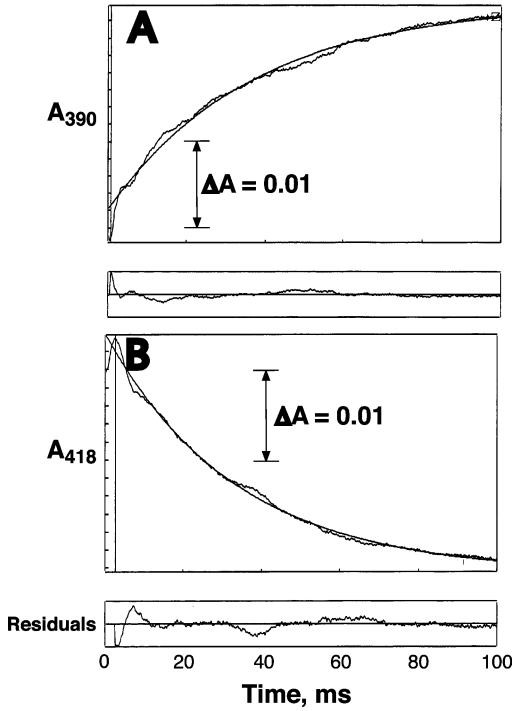

FIGURE 1: Kinetics of substrate binding. P450 1A2 (4 μM, with 50 μM di-12:0 GPC but no NADPH−P450 reductase) was mixed rapidly with αNF (40 μM) in 0.10 M potassium phosphate buffer (pH 7.4) at 26 °C. The traces at 390 nm (A) and 418 nm (B) are shown and are fit to a single-exponential equation, yielding first-order rates of 27 s^{-1} and 30 s^{-1} for the two points (each curve represents an average of eight individual analyses).

analyzed by HPLC using the procedure described for steady-state reactions (vide supra).

Kinetic Simulation and Modeling. The program DynaFit (*62*) was used to develop and fit sets of rate constants to models. General approaches are discussed elsewhere (*19*, *63*), and some sample scripts and files are attached as Supporting Information.

RESULTS

A series of studies was used to analyze individual reaction steps (Scheme 1). The approach to this kinetic analysis consists of experimental measurements of individual rate constants, a set of kinetic deuterium isotope effect studies, spectral examination of a reaction in the steady state, and fitting to kinetic models and rate constants, plus analysis of the effects of changing rates of individual steps.

Substrate Binding (Step 1 of Scheme 1). Binding of some substrates to rabbit P450 1A2 induces a shift of the heme iron from the low- to the high-spin form (*45*, *50*). Of a series of ligands examined, the most effective was αNF (*45*), a tightly bound ligand and slowly oxidized substrate. The rate constant measured at a substrate concentration of 5 μM was 1600 min^{-1}, indicating a rate of $\geq 5 \times 10^6$ M^{-1} s^{-1} (Figure 1). We assume that this rate is representative for other substrates, and we conclude that it is not rate-limiting. (Because the rate of this step was not limiting, we did not proceed to examine substrate concentration dependence.)

Product Release (Step 7 of Scheme 1). If events following the formation of product are rate-limiting, the reaction progress is observed as a kinetic "burst" (*17*, *39*, *64*). We previously demonstrated that steps prior to product formation

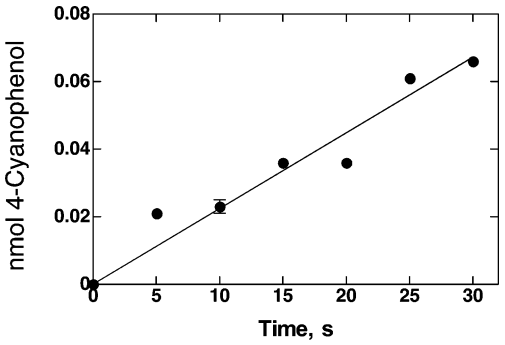

FIGURE 2: Lack of burst kinetics in P450 1A2-catalyzed 4-cyanoanisole O-demethylation. The experiments were done with 0.5 nmol of P450 1A2 and 1.0 nmol of NADPH−P450 reductase plus other components mentioned in Experimental Procedures [Enzyme Reactions (Steady State)] at 23 °C, and the resulting 4-cyanophenol was analyzed by HPLC. The resulting data points were fit to a linear regression plot.

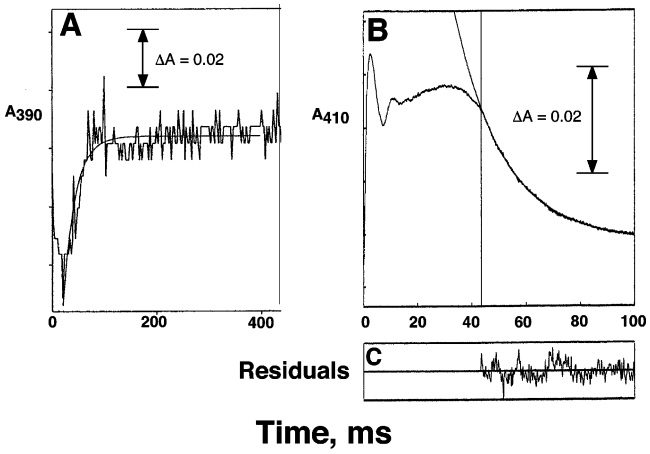

FIGURE 3: Reaction of ferrous P450 1A2 with O_2 to form FeO_2^{2+}. P450 1A2 (20 μM, with 150 μM di-12:0 GPC and 23 μM αNF) was reduced photochemically (using 5-deazaflavin) and mixed with air-saturated buffer (all buffers 0.10 M potassium phosphate, pH 7.4, with 50 mM Tris·HCl and 10 mM EDTA in P450 1A2 tonometer/syringe to provide electrons for photoreduction) at 25 °C. (A) A_{390} trace (from data collected using a diode array detector of the Applied Photophysics instrument). (B) A_{410} trace (single wavelength setting). The plots in parts A and B are fit to single exponentials of 43 s^{-1} and 57 s^{-1}, respectively, and the residual analysis is shown in part C (not available for part A because of the detection system used).

are rate-limiting in reactions catalyzed by human P450 1A2 (*40*), and no kinetic burst was observed for the O-demethylation of 4-cyanoanisole by rabbit P450 1A2 (Figure 2). In other experiments, no burst was seen in the O-demethylation of 7-methoxyresorufin by rabbit P450 1A2 (results not shown). The structures of this substrate and 4-cyanoanisole are rather different, and we presume that this lack of a kinetic burst will be a general phenomenon.

Rate of O_2 Binding (Step 3 of Scheme 1). Ferrous P450 1A2 (αNF complex) was reacted with O_2 and a very rapid spectral change occurred, following a lag phase of ~40 ms, due to an artifact related to oxidation of the reduced dye. Analysis of some of the changes yielded rates of 2600 min^{-1} (ΔA_{390}) to 3400 min^{-1} (ΔA_{410}) (Figure 3). These rates, measured with air-saturated buffer in the second syringe (i.e., $[O_2] \cong 100$ μM), indicate a rate of $\geq 5 \times 10^5$ M^{-1} s^{-1}. (Because this step is clearly not limiting, we did not examine the rate as a function of O_2 concentration.)

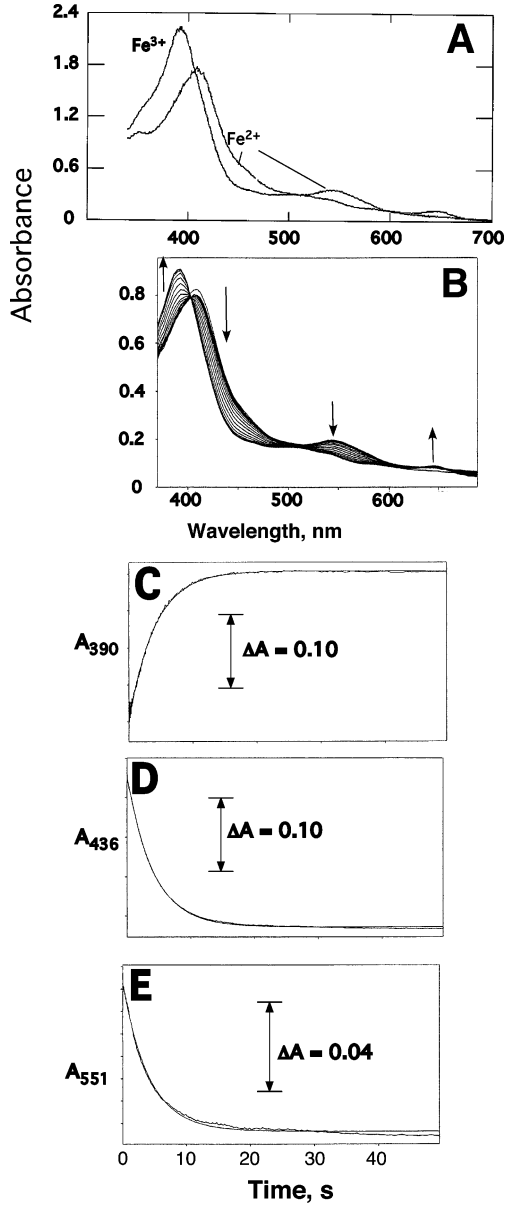

FIGURE 4: Spectra of Fe^{3+} and Fe^{2+} P450 1A2 and decay of the FeO^{2+} complex. (A) P450 1A2, conditions as described in Figure 3. Fe^{3+}, ferric form. Fe^{2+}, ferrous form (photoreduced). Spectra were recorded anaerobically in an OLIS/Cary 14 instrument. (B) Spectra following mixing of ferrous P450 1A2 with air-saturated buffer. The first trace was collected (diode array) at 0.5 s, following the changes reported in Figure 3. (C−E) Changes in absorbance at 390, 436, and 551 nm. All traces were fit to a single exponential of 0.24 s^{-1} (14 min^{-1}).

Decay of the $Fe^{2+}-O_2$ Complex. As indicated in the previous section, the reaction of ferrous P450 1A2 with O_2 yielded a rapid change to a new spectral complex that was distinct from the Fe^{2+} (or Fe^{3+}) entity (Figure 4A, B). The O_2-bound complex (Figure 4B) is similar to the Fe^{2+} form of the enzyme (Figure 4A), with a λ_{max} at slightly shorter wavelength (409 nm), but cannot be the same because of (i) the ratio of the Soret band to the that of the Fe^{3+} complex, which varies (Figure 4A), and (ii) the observation of rapid changes occurring before decay of the new complex, as reported in Figure 3. The reaction proceeded with an isosbestic change of the spectra, at a rate of 14 min^{-1} (at 25 °C) (Figure 4B−E). The final spectrum was that of the ferric enzyme.

Limited Cycle Experiments. P450 1A2 (45 nmol) was mixed with an equivalent amount of NADPH−P450 reductase, and a stoichiometric amount of NADPH (calibrated by A_{340} measurement) was added (135 nmol, 2 electron equivalents per P450 reaction and 4 electron equivalents per reductase), in the presence of the substrate methacetin, one of the better substrates for rabbit P450 1A2 (vide infra). The yield of products was 38 nmol (28%) (Figure 5, Table 1). The experiment was also done with sequential deaeration of the enzymes, anaerobic reduction with NADPH, and then reaction with O_2, yielding a 59% yield of the products. A third experiment involved photochemical reduction of P450 1A2 (anaerobically) in the presence of 5-deazaflavin, followed by addition of O_2 (i.e., conditions similar to those used in the spectral studies in Figure 4). The yield of product was 61%, based on the calculations with 1 electron/P450 plus correction for the deazaflavin. Interestingly, the pattern for the two products (acetaminophen and acetol) was more similar to the steady-state experiments in the single-turnover experiments done with only P450, as opposed to having NADPH−P450 reductase present and using NADPH (i.e., relatively more acetol formed in the presence of reductase and NADPH; Figure 5 and Table 1).

Kinetic Deuterium Isotope Effects. Kinetic isotope effect studies can provide valuable information about the relative rates of individual steps within a complex catalytic cycle. Several types of experiments were used (Scheme 2, Table 2).

The apparent intrinsic deuterium isotope effects (^{D}k) (*intramolecular noncompetitive*) were high, varying from 7.0 to 14.7 (Table 2). The selection for breaking a C−H vs a C−D bond of a methyl group is limited only by bond strengths because of the rapid rotation of a methyl group, and prochirality is not an issue as in the case of methylene substrates. In principle, these are the maximum isotope effects (although uncorrected for any contribution of secondary isotope effects), and all others should be compared to judge the extent of attenuation due to rate-limiting steps.

An *intramolecular competitive* experiment was done with the substrate 1,4-dimethoxybenzene, which has equivalent methoxy groups, yielding an isotope effect [$^{D}(V/K)$] of 4.1 (Table 2). This value is attenuated from the intrinsic ^{D}k (8.4) but is still very significant. In principle, this value provides information about the ability of the molecules to tumble within the active site while the activated P450 complex (FeO^{3+}) is functional, although the intermolecular isotope effect of 3.1 renders this interpretation tentative. The (d_3) substrate could also be replaced by another molecule of the substrate (d_0); i.e., the result can be influenced by the phenomena that result from an intermolecular competitive experiment (Scheme 2D), because a similar value was obtained in each case (Table 2).

The *intermolecular noncompetitive* isotope effects (Scheme 2A) were determined and provide insight into the degree to which the C−H bond-breaking step is rate-limiting. Although these measurements are most subject to issues of substrate purity and propagation of statistical error by their very nature (*3*), they also provide the most direct information as to what degree the C−H bond-breaking step is rate-limiting in the overall steady-state reaction. These isotope effects, both ^{D}V and $^{D}(V/K)$, were generally high, with those for 4-nitroanisole and 4-cyanoanisole approaching the estimated

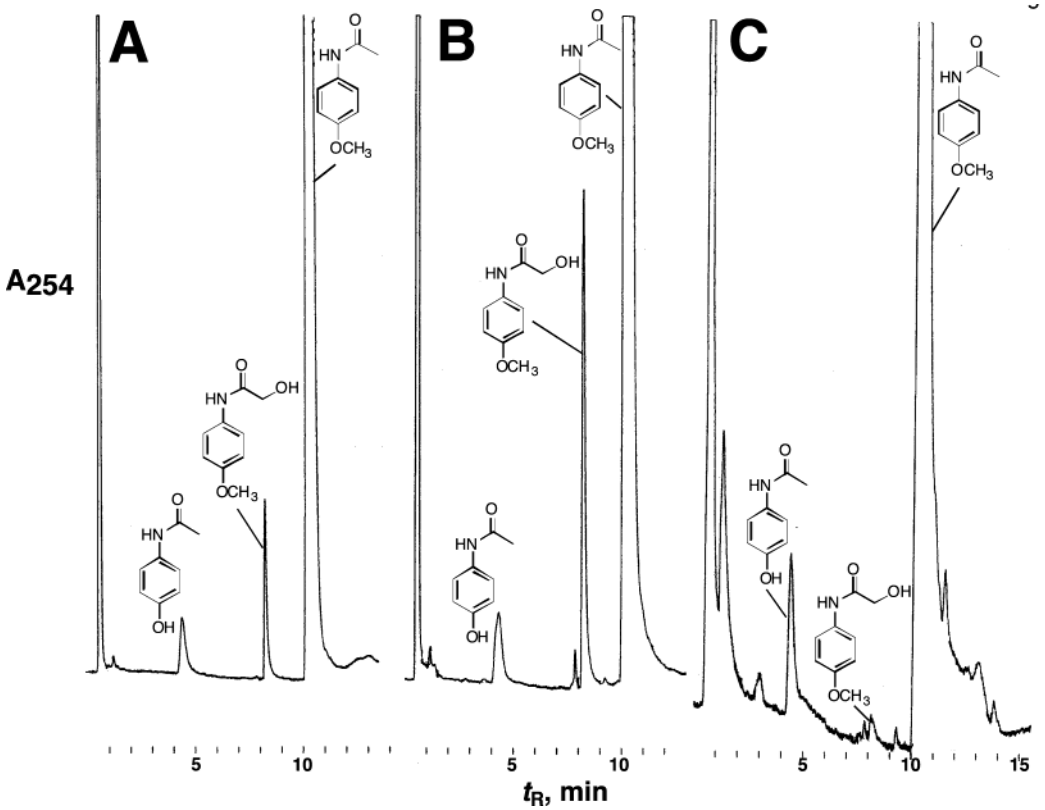

FIGURE 5: Conversion of methacetin to products by P450 1A2 in single-turnover experiments. See text and Table 1 for a description and details of experiments. (A) Reduction using reductase and NADPH in an aerobic experiment. (B) Reduction using reductase and NADPH to reduce P450 anaerobically, followed by mixing with air. (C) Photochemical reduction of P450 1A2 (anaerobically) in the absence of reductase, followed by mixing with air. The peaks were identified by comparison with t_R values of external standards.

Table 1: Product Formation in Single-Turnover Reactions[a]

components	order of treatment	total reduction equivalents	methacetin product (nmol)		
			phenol	acetol	total
P450 1A2,[b] NADPH−P450 reductase[c]	$+O_2$, +NADPH	135 nmol of NADPH	26	12	38 (28%)
P450 1A2,[b] NADPH−P450 reductase[c]	$-O_2$, +NADPH, $+O_2$	135 nmol of NADPH	42	38	80 (59%)
P450 1A2,[b] 5-deazaflavin[d]	$-O_2$, $+1e^-$ ($h\nu$),[e] $+O_2$	45 nmol of P450	16	0.7	16.7 (61%)[f]

[a] Total volume 3.0 mL. [b] 45 nmol of P450 1A2. [c] 45 nmol of NADPH−P450 reductase. [d] Added at 5 μM (total 15 nmol), plus 1 μM safranine T as an indicator for reduction. [e] Photoreduction. [f] $16.7/[(45/2) + 5] = 16.7/(22.5 + 5) = 16.7/27.5 = 0.61$, based on $2e^-$/deazaflavin and the requirement for $2e^-$ needed to form one product/P450.

Table 2: Kinetic Deuterium Isotope Effects on Rabbit P450 1A2 Reactions

substrate	product	k_{cat} (min^{-1})	kinetic deuterium isotope effect[a]				
			intramolecular (noncompetitive, intrinsic) ^Dk	intermolecular (noncompetitive) ^DV	intermolecular (noncompetitive) $^D(V/K)$	intermolecular (competitive) $^D(V/K)$	intramolecular (competitive) $^D(V/K)$
4-nitroanisole	4-nitrophenol	1.3	14.7 (±2.0)	14.4 (±1.6)	14.9 (±2.1)	8.1 (±0.4)	nd[b]
4-cyanoanisole	4-cyanophenol	2.0	8.4 (±1.4)	7.9 (±0.5)	8.4 (±1.5)	7.7 (±0.9)	nd[b]
1,4-dimethoxybenzene	4-hydroxyanisole	3.4	8.4 (±0.7)	5.8 (±0.8)	4.5 (±0.6)	3.1 (±0.2)	4.1 (±0.2)
methacetin	acetaminophen	31.5	7.0 (±0.2)	2.4 (±0.1)	1.9 (±0.1)	1.9 (±0.1)	nd[b]
	acetol	0.19	5.8 (±0.1)[c]	—[d]	7.6 (±2.5)[d]	nd[b]	
7-methoxyresorufin	7-hydroxyresorufin	1.1	nd[b]	7.4 (±0.6)	3.9 (±0.3)	nd[b]	

[a] See Scheme 2 for a description of experimental designs. SE in parentheses. [b] Not determined. [c] A parallel experiment with [*acetamido-d*$_1$]phenacetin yielded a value of 7.1 ± 0.7. [d] $^Dk_{cat}$ was too low to permit accurate quantitation with the d_3 substrate for this reaction. The ratios of k_{cat}/K_m were estimated from the slopes of plots of v vs S.

intrinsic ^Dk values. These results argue that C−H bond breaking is very rate-limiting in these reactions. The isotope effects for 1,4-dimethoxybenzene were lower than the ^Dk but still high (>5). The previously reported human P450 1A2 isotope effects for O-dealkylation (*40*) are also low relative to the ^Dk (for the C−H bond-breaking step). With regard to formation of the acetol, a minor pathway (but see Table 1), the ^Dk was similar to that observed for O-demethylation, and the $^D(V/K)$ was not attenuated [the sensitivity of the assay did not allow for a reliable estimate of ^DV, but $^D(V/K)$ could be estimated from the slopes of v vs S plots].

The *intermolecular competitive* isotope effects [$^{D}(V/K)$] were measured and were similar to the $^{D}(V/K)$ values obtained in the noncompetitive experiments (for 4-cyanoanisole and methacetin O-demethylation) or somewhat lower (4-nitroanisole and 1,4-dimethoxybenzene). In the design of these experiments (Scheme 2D), a high intrinsic isotope effect (^{D}k) is suppressed if the rates of exchange of C−H and C−D substrates are slow relative to C−H bond breaking (*3*). That is, a high catalytic commitment (*3*) will allow an enzyme to proceed with catalysis of a C−D substrate before enough time elapses to discard it in favor of a C−H substrate; a lower isotope effect will be observed. The lack of attenuation in this set of experiments (Table 2) is consistent with the direct measurement of a rapid k_{on} rate (step 1 of Scheme 1) (Figure 1) and a lack of burst kinetics (step 7 of Scheme 1) (Figure 2).

This latter set of experiments was designed to examine the ability of an enzyme to sense the energetic challenge of breaking a C−H bond late in the catalytic cycle or opt to bind a new substrate before performing catalysis (Scheme 2D). One option is for the P450 to retain the reactive FeO^{3+} entity while the deuterated product dissociates and a protiated substrate enters the binding site; the other is for the FeO^{3+} intermediate to collapse (to Fe^{3+}) and begin the catalytic cycle again, with protiated substrate instead of a deuterated one. To discriminate between these two possibilities, an experiment was done in which the total production of the product was measured (Figure 6A). If the commitment of the reaction were such that the FeO^{3+} complex could readily exchange a protiated substrate for the deuterated one, we would expect the same k_{cat} for a 1:1 mixture of d_0/d_3 substrate as for the d_0 substrate. However, the pattern we observed had the mixture of d_0/d_3 substrate giving a k_{cat} almost exactly intermediate between the separate plots for d_0 and d_3 (Figure 6A). Thus the d_3 and d_0 substrates appear to exhibit independent behavior and support the model (Scheme 2D) in which the FeO^{3+} complex cannot persist while substrates dissociate and associate, at least in the case of 4-cyanoanisole. Further evidence for this conclusion was obtained in a study in which the rate of O-demethylation of this substrate was measured with substrate mixtures of varying deuterium content (Figure 6B). The linear fit implies the independence of the routes with d_0 and d_3 substrates.

Other Kinetic Hydrogen Isotope Effects (7-Methoxyresorufin). The above kinetic isotope effects were determined in systems containing an optimal amount of NADPH−P450 reductase. The question can be raised as to how much C−H bond breaking is rate-limiting in a more biological system such as liver microsomes, where the ratio of the reductase:P450 is ∼1:20 (*65*). For this assessment we used 7-methoxyresorufin O-demethylation, which has been generally accepted as a relatively specific marker reaction for P450 1A2 reactions, even among several species (*66*, *67*). With purified rabbit P450 1A2, intermolecular noncompetitive isotope effects of $^{D}V = 7.4$ and $^{D}(V/K) = 2.5$ were measured ($k_{cat} = 1.1$ min^{-1}). A purified rat P450 1A2 system (*53*) yielded $k_{cat} = 1.0$ min^{-1}, $^{D}V = 3.2$, and $^{D}(V/K) = 2.6$. Liver microsomes prepared from rats treated with the inducer 7,8-benzoflavone (*53*) yielded $k_{cat} = 0.63$ min^{-1} (based on total P450), $^{D}V = 6.5$, and $^{D}(V/K) = 3.2$. Thus, the isotope effect results suggest that the isotope effect for this reaction is not suppressed by the limited amount of NADPH−P450 reductase in microsomes and that C−H bond breaking, in this case, is probably relevant in the liver itself.

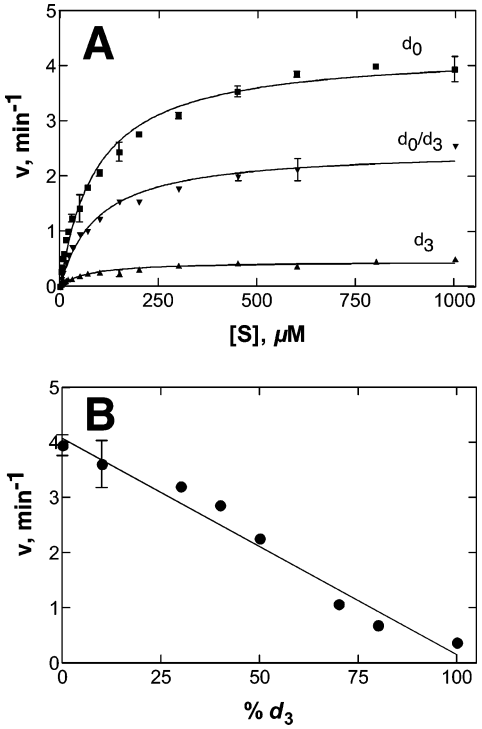

FIGURE 6: Intermolecular noncompetitive and competitive kinetic deuterium isotope effect studies of P450 1A2-catalyzed O-demethylation of 4-cyanoanisole. (A) Steady-state experiments were done with d_0, d_3, or a 1:1 molar ratio mixture of d_0 and d_3 4-cyanoanisole, and the formation of 4-cyanophenol was measured using HPLC. The following parameters were measured: for d_0, k_{cat}, 4.3 (±0.1) min^{-1}; K_m, 9.2 (±8) μM; k_{cat}/K_m, 47 × 10^{-3} min^{-1} M^{-1}; for d_3, k_{cat}, 0.46 (±0.02) min^{-1}; K_m, 69 (±10) μM; k_{cat}/K_m, 6.7 × 10^{-3} min^{-1} M^{-1}; for mixture of d_0/d_3, k_{cat}, 2.5 (±0.1) min^{-1}; K_m, 93 (±9) μM; k_{cat}/K_m, 27 × 10^3 min^{-1} M^{-1}; ^{D}V, 9.3; $^{D}(V/K)$ 7.0. (B) The same experiments were done as in part A, except that the total 4-cyanoanisole concentration was set at 1.0 mM, the fraction of d_3 4-cyanoanisole was adjusted as indicated, and the rate of 4-cyanophenol formation was determined. The data points were fit to a linear regression curve.

Steady-State Spectral Analyses. One means of obtaining information about rate-limiting steps is the examination of accumulated spectral species in steady-state reactions. A reconstituted system consisting of P450 1A2, NADPH−P450 reductase, di-12:0 GPC, and the substrate methacetin was mixed with NADPH (and an NADPH-generating system). The first spectral trace indicated the oxidized P450 and NADPH−P450 reductase (as revealed by the flavin absorbance band remaining from 450 to 500 nm) (Figure 7). The spectrum changed quickly ($k = 1140$ min^{-1}, single exponential at 461 nm) (Figure 7B) (also, single exponential $k = 1380$ min^{-1} for the decrease of absorbance at 438 nm; not shown) to one that persisted for at least 5−10 min (Figure 7C). The λ_{max} is similar to but does not correspond exactly to that observed for the FeO_2^{2+} complex (Figure 4), with a slightly higher λ_{max} (red shifted), and the identity of this species (or mixture of species) is discussed later.

Fitting of Steady-State Kinetic Data to Mechanisms. A simplified mechanism was developed (Scheme 3). In this system, the conversion of ES (P450 Fe^{3+}−substrate) to FSO [P450 $(FeO)^{3+}$−substrate complex] is treated as a single step. The isotopically sensitive step, which involves the C−H

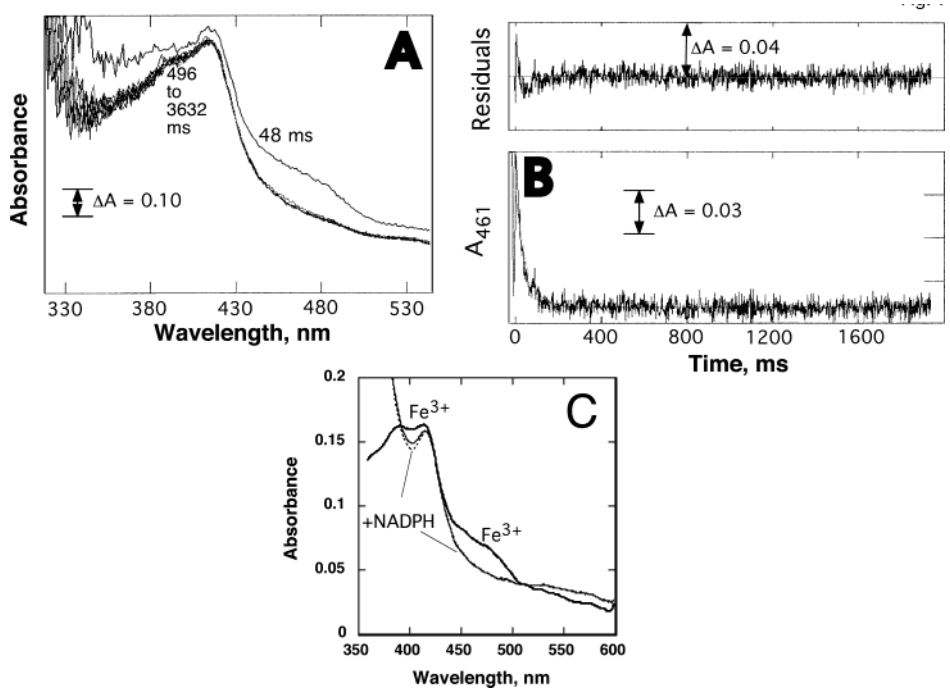

FIGURE 7: Steady-state spectra of P450 1A2 during turnover. One syringe of a stopped-flow spectrophotometer (OLIS RSM-1000) contained P450 1A2 (10 μM), NADPH−P450 reductase (15 μM), di-12:0 GPC (45 μM), methacetin (200 μM), and potassium phosphate buffer (0.10 M, pH 7.4). The other syringe contained 50 μM NADPH, 5 mM glucose 6-phosphate, and 1 IU of yeast glucose 6-phosphate dehydrogenase mL^{-1} in 0.10 M potassium phosphate buffer (pH 7.4) (both syringes were saturated with air, at 25 °C). The syringes were mixed, using a slit width of 3.16 mm and a band-pass of 20 nm. (A) A_{480} trace, fitted to a single-exponential plot with $k = 19$ s^{-1}. Spectra were recorded (rapid-scanning monochromator) immediately ($t = 48$ ms) and then at the rate of 62 s^{-1} over the range 496−3632 ms. The traces shown are 1 of every 14 collected. (B) Fit of the A_{461} trace to a single exponential, $k = 19$ s^{-1} (1140 min^{-1}). Analysis of the decrease at 438 nm (not shown) yields a single exponential of 23 s^{-1} (1380 min^{-1}). (C) A similar experiment was done with 1.0 μM P450 1A2 and 1.5 μM NADPH−P450 reductase, with manual addition of NADPH and conventional scanning in an OLIS-Cary 14 spectrophotometer. The system was scanned respectively for 10 min (23 °C), and the traces all overlaid the patterns of the two shown here ($t = 5$ and 10 min, indicated with +NADPH).

Scheme 3: Abbreviated Scheme of P450 Catalysis for Kinetic Simulations[a]

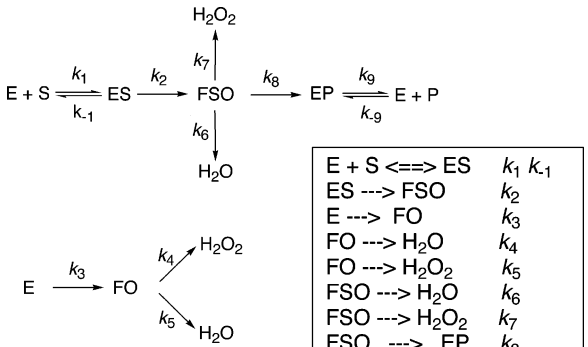

E + S <==> ES	k_1 k_{-1}
ES ---> FSO	k_2
E ---> FO	k_3
FO ---> H_2O	k_4
FO ---> H_2O_2	k_5
FSO ---> H_2O	k_6
FSO ---> H_2O_2	k_7
FSO ---> EP	k_8
EP <==> E + P	k_9 k_{-9}

[a] E = P450, S = substrate, FSO = P450−substrate complex, with iron in the oxidized state for catalysis, FO = oxidized P450 with iron in form(s) that yield(s) the reduced oxygen species H_2O_2 and H_2O, and P = product. See text and Table 3 for analysis of rate constants and fitted values.

bond-breaking step, is designated k_8. The production of H_2O_2 and apparently H_2O (calculated by difference following determination of NADPH oxidation and H_2O_2 production rates) occurs in the absence of substrate. Because NADPH oxidation (and apparently H_2O formation) increased with substrate (4-cyanoanisole) concentration in this study, both FO and FSO (Scheme 3) are treated as capable of yielding H_2O and H_2O_2.

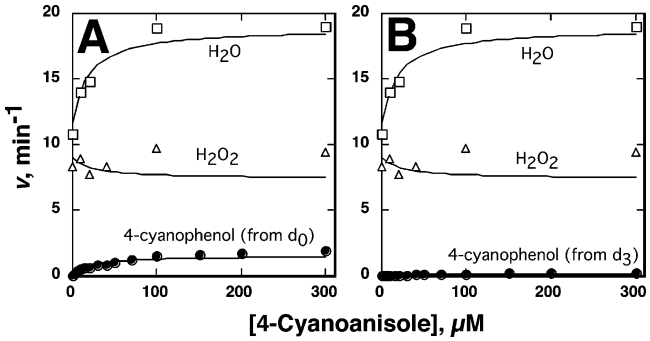

FIGURE 8: Fits to P450 1A2 kinetic data using simulated rate constants. The data points indicate the rates of formation of 4-cyanophenol (●), H_2O_2 (△), and H_2O (□) at varying 4-cyanoanisole concentrations. (A) d_0 4-cyanoanisole. (B) d_3 4-cyanoanisole. The plots (solid lines) were fit with the mechanism and rate constants presented in Table 3.

Fitting of the steady-state results for the O-demethylation of 4-cyanoanisole (both d_0 and d_3) plus the production of H_2O_2 and H_2O is shown in Figure 8, with the values of a set of individual rate constants that can provide a reasonable fit to the data listed in Table 3.

DISCUSSION

A number of approaches were used to evaluate the rate-limiting nature of steps within the catalytic cycle of rabbit P450 1A2 reactions. These studies indicate that the rate-limiting step in most of the reactions studied is during or prior to product formation but after the formation of the

Table 3: Rate and Equilibrium Constants Used in Fitting Plots of Steady-State O-Demethylation of 4-Cyanoanisole

rate constant[a]	value	other
k_1	6×10^9 M^{-1} min^{-1}	$K_d = 17$ μM
k_{-1}	10^5 min^{-1}	
k_2	220 min^{-1} [b]	
k_3	190 min^{-1} [b]	
k_4	35 min^{-1}	
k_5	45 min^{-1}	
k_6	63 min^{-1}	
k_7	160 min^{-1}	
k_8 (for d_0)	13 min^{-1}	$^Dk = 11$
k_8 (for d_3)	1.2 min^{-1}	
k_9	2.4×10^5 min^{-1}	$K_d = 40$ μM
k_{-9}	6×10^9 M^{-1} min^{-1}	

[a] Scheme 3. [b] For reference to rates of 1-electron reduction (of ferric P450) see ref *68*. See also Figure 7.

$Fe^{2+}-O_2-$substrate complex, i.e., steps 4−6 of Scheme 1. Steps 1 and 3 were all measured directly and found to be rapid, step 2 was previously shown to be rapid [with or without substrate present (*68*)], and step 7 is rapid as judged by the absence of a kinetic burst (Figure 2). The limited attenuation of the high ^Dk in several reactions (Table 2) indicates a highly limiting C−H bond-breaking step in those cases.

Our conclusions are that the rate-limiting steps involve reaction of the substrate with oxygenated iron complexes. This conclusion is based on (i) the high rates of reaction measured for steps 1−3, (ii) the significant noncompetitive intermolecular isotope effects observed in all cases examined (Table 2), and (iii) the accumulation of spectral intermediates during the reaction steady state (Figure 7). In some cases the full expression of the high intrinsic kinetic isotope effects (Table 2) argues that the C−H bond-breaking step is almost fully rate-limiting. We are unable to assign the chemical nature of the spectral complex that accumulates in the steady state (Figure 7). The Soret band does not exactly match that of either the Fe^{3+}, Fe^{2+}, or apparently FeO_2^{2+} forms (Figure 4). Thus a case can be made that none of steps 1−4 or 7 of Scheme 1 is completely rate-limiting, narrowing the possibility to steps 5 and 6, although there are more possibilities than only the formal FeO_2^{2+} and FeO^{3+} entities. A problem with further efforts to assign the spectral complex is that the steady state may well contain a mixture of different species. The formation of H_2O_2 and, by inference (*57*), H_2O (Figure 8) indicates that steps 8 and 9 of Scheme 1 (or alternative routes to these reduced oxygen products) are occurring and confounding the analysis of the pathway leading to product. Further, the yields of products in the single-turnover experiments were less than quantitative.

An interesting aspect of this work was the limited cycle experiments (Figures 4 and 5, Table 1). Oprian et al. (*69*) formed the $Fe^{2+}-O_2$ complex of rabbit P450 1A2 (then termed $P450_{LM4}$) in the absence of substrate. The complex decomposed to yield H_2O_2 in 70% yield, without any accumulation of $O_2^{\bullet-}$ (we did not quantify H_2O_2 in our experiments; Table 1). Oprian et al. (*69*) fit the decay to a biexponential plot ($k = 55$ and 13 min^{-1} at 10 °C), with no apparent intermediate in the decay to the Fe^{3+} form. In our experiments (Figure 4), the isosbestic decay (at 23 °C) fit very well to a single exponential (these data were collected in the presence of the substrate αNF). Under similar conditions with the substrate methacetin, a yield of 61% product (mainly from O-demethylation) was obtained (Table 1). The calculation of the yield is based upon the use of 2 electrons per product; two $Fe^{2+}-O_2-$methacetin complexes must interact to provide the appropriate transfer of electrons to one of them for product formation [i.e., $2(Fe^{2+}-O_2-$substrate) → $Fe^{3+}-$substrate + H_2O + $FeO^{3+}-$substrate → Fe^{3+} + product]. Thus, the results implicate P450-to-P450 electron transfer. The yield of total product was similar to that seen in an experiment where NADPH−P450 reductase was also present and the electrons entered the system from NADPH (Table 1). Fully reducing both flavins in the reductase would require 4 electrons; we do not have an analysis of how many electrons remained in the final form of the flavoprotein after transfer. A desirable experiment would involve the mixing of NADPH−P450 reductase with a P450 $Fe^{2+}-O_2-$substrate complex and monitoring of spectral changes and product formation; however, the binding of the two proteins to form a productive complex is a relatively slow process (*68*). Surprisingly, the product ratio resembled that obtained in steady-state reactions (Table 2) more closely in the case of the system with only P450 than the system containing both P450 and NADPH−P450 reductase (Figure 5, Table 1). Relatively few such limited cycle or equivalent studies have been done with P450s other than bacterial P450 101 (*70*, *71*), and the relatively good yields suggest that more detailed investigations of kinetics may be in order.

We have considered the kinetics of individual reaction steps in the context of a simplified kinetic model (Scheme 3), in which all events leading from the $Fe^{3+}-$substrate complex (devoted ES) to the full activated P450 species FSO (putatively FeO^{3+}) are grouped together and represented by an overall rate constant, k_2. A global fitting to the three sets of data points in each part of Figure 8 (with only k_8 allowed to vary between the d_0 and d_3 4-cyanonanisole experiments) yielded the fits shown with the set of parameters shown in Table 3. The values are not necessarily unique but do provide a reasonable estimate. The calculated isotope effect on step k_8 is 11, in reasonable agreement with the apparent ^Dk of 8.4 measured experimentally with d_2 4-cyanoanisole (Table 2). It should be emphasized that values for steps other than k_8 could be adjusted to other values and still yield fits to the product curves (except k_1, k_{-1}, k_9, and k_{-9}). However, adjustment of the other values to those presented in Table 3 provided a superior fit to the H_2O_2 and H_2O results, which is a critical issue in the fitting process.

The simplified model of Scheme 3 and the values presented in Table 3 provide a reasonable fit to the data set used in Figure 8. This is not necessarily a unique solution, and the model used (Scheme 3) is certainly an oversimplification. In principle, a more complex mechanism (Scheme 1) would even have to be expanded to include substrate dissociation at intermediate steps (although apparently not at the FeO^{3+} complex; Figure 6). Despite the caveats associated with the modeling, the information can be used to make some inferences and predictions about the system.

Using the parameters presented in Table 3 and the system of Scheme 3, the effects of varying k_8, which appears to be a rate-limiting step in all of these reactions of P450 1A2 we have studied here, may be predicted (Figure 9). k_{cat} and k_{cat}/K_m, the catalytic efficiency, both increase to asymptotes at

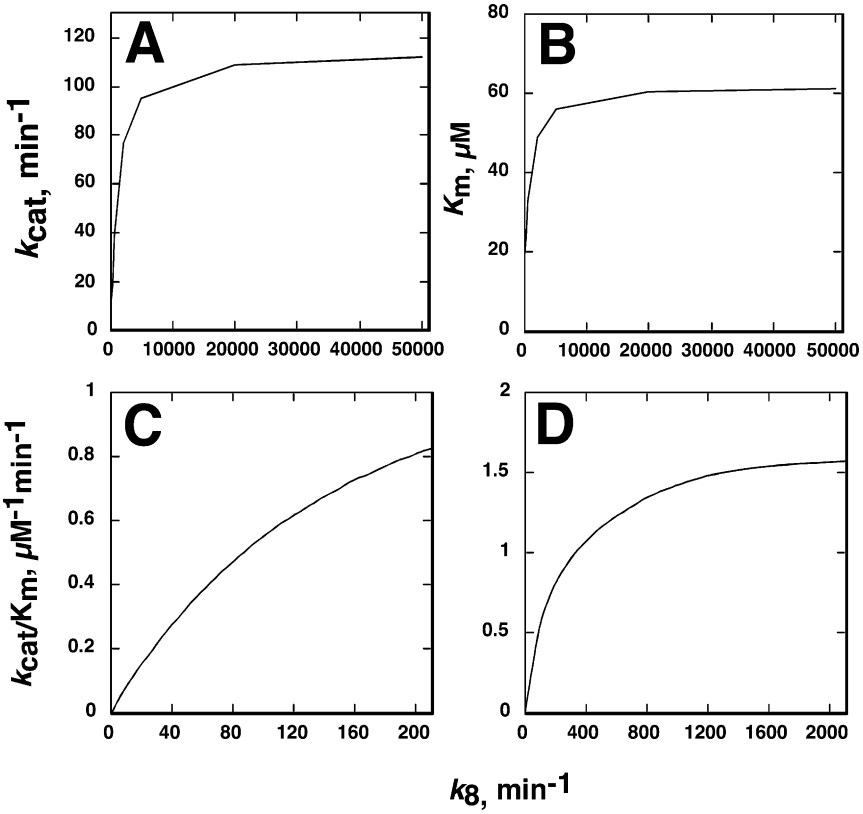

FIGURE 9: Effects of changing k_8 (C−H bond-breaking step) in a kinetic model. The mechanism and rate constants presented in Table 3 were used, with only k_8 varied. The plots show the effects of varying k_8.

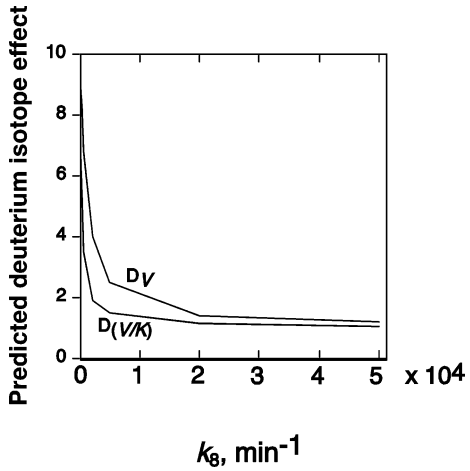

FIGURE 10: Effect of varying k_8 (C−H bond-breaking step, Scheme 3) on kinetic deuterium isotope effects.

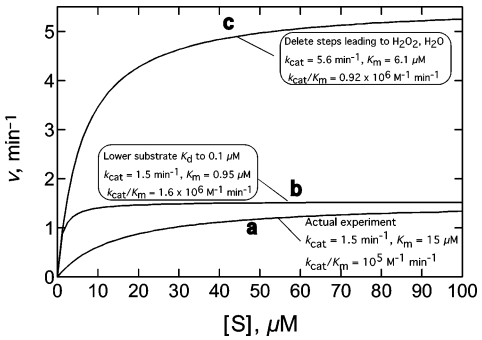

FIGURE 11: Simulations of mechanisms and effects of attempts to improve catalytic efficiency. The experimental system (actual data) yielded $k_{cat} = 1.5$ min^{-1}, $K_m = 15$ μM, and $k_{cat}/K_m = 1 \times 10^5$ M^{-1} min^{-1} for the O-demethylation of 1,4-dimethoxyanisole (points not shown, for clarity). The effect of lowering K_d, the actual substrate binding constant (ferric P450), to 0.1 μM is shown ($k_{cat} = 1.5$ min^{-1}, $K_m = 0.95$ μM, $k_{cat}/K_m = 1.6 \times 10^6$ M^{-1} min^{-1}). Complete suppression of pathways leading to abortive oxygen reduction yields $k_{cat} = 5.6$ min^{-1}, $K_m = 6.1$ μM, and $k_{cat}/K_m = 9 \times 10^5$ M^{-1} min^{-1}.

$k_8 \sim 5 \times 10^3$ min^{-1}. The maximum k_{cat} is $\sim$110 min^{-1}, so at this point C−H bond breaking is no longer rate-limiting. The predicted effect on the observed intermolecular noncompetitive isotope effect is shown in Figure 10 and is consistent with the report of Kadkhodayan et al. (*37*) with different substrates of bacterial P450 101. Steps other than C−H bond breaking need to be enhanced to obtain rates >110 min^{-1} (Figure 9). Even though the substrate K_d (k_{-1}/k_1) is unchanged, K_m increases with k_8 (Figure 9), showing the catalytic complexity of the system (4-fold change in going to $k_8 \sim 5 \times 10^3$ min^{-1}).

The options for modifying a P450 reaction are considered further in Figure 11. As indicated in Figure 9, one means of increasing the catalytic efficiency is to increase k_8, the "chemical" reaction step (C−H bond breaking or its equivalent). A commonly discussed means of increasing the activity of a P450 is the goal of using molecular modeling/site-directed mutagenesis to improve the bonding of substrate. Lowering the ground-state K_d (defined here as k_{-1}/k_1), apart from any other steps, may increase the catalytic efficiency (k_{cat}/K_m) but not necessarily the k_{cat} (Figure 11). Of interest is our prediction that both the k_{cat}/K_m and the k_{cat} could be remarkably improved by attenuation of the steps leading to H_2O_2 and H_2O (Figure 11) (interestingly, this exercise also shows a decrease in K_m).

Not only Scheme 3 but even Scheme 1 is an oversimplification of the P450 reaction mechanism. One of the deficiencies of this model (Scheme 1), as it is usually

presented, is that substrate binding (and dissociation) is usually shown only in step 1. However, substrates can bind reversibly to ferrous P450, and we showed that a ligand for P450 3A4 had different K_d values with the ferric and ferrous enzymes (*72*). We examined the possibility that substrate could exchange at the step just before C−H bond breaking (Scheme 2D), but the results suggest that the exchange of substrate with the putative FeO^{3+} entity is very limited, if it occurs at all. Blocking the path to C−H bond breaking causes the activated intermediate (FeO^{3+}) substrate complex to collapse. In one sense this result might seem inconsistent with the apparent "ping-pong" mechanisms observed with oxygen surrogates such as hydroperoxides and iodosylbenzene (*73*, *74*). However, many of the reactions observed with hydroperoxides and peracids may use alternate mechanisms [e.g., FeO^{2+}/RO• (*75*)], and some of the iodosylbenzene reactions may use a bound Fe−O−PhI species (*76*, *77*). We propose that substrate can probably exchange at the species found between Fe^{2+} and FeO^{3+} in Scheme 1, in that the off rates are probably very high [e.g., a K_d of 10^{-5} M and $k_{on} = 10^8$ M^{-1} s^{-1} (Table 3) gives a k_{off} of 10^3 $s^{-1} = 6 \times 10^4$ min^{-1}]. However, a series of pulse−chase experiments is in order to prove the hypothesis about exchange of ligands in steps at FeO_2^{2+} and beyond. The expected effect of such dissociations would be to modify the K_m.

The high kinetic deuterium isotope effects (Table 2) merit further consideration. Values >10 are not unprecedented in P450 reactions (*27*, *38*, *40*, *78*). Studies with bacterial P450 101 indicate that although the intrinsic kinetic hydrogen isotope effects are not known with certainty [due to issues with the stereochemistry of abstraction at a chiral methylene (*35*)], the expressed isotope effect on camphor 5-*exo* hydroxylation is small (*35*) but increases with modified substrates that are not oxidized as rapidly (*36*, *37*). In the case of 1(*R*)-5,5-difluorocamphor 9-hydroxylation, the expressed isotope effect was 11.7 (*37*), and the hydroxylation rate was only 3% that for 1(*R*)-camphor 5-*exo* hydroxylation. Thus, there is a shift of the rate-limiting step from reduction (*79*) to C−H bond breaking, consistent with predictions such as the exercise shown in Figure 10.

The high isotope effects seen with some of the bacterial and mammalian P450 enzymes are greater than the generally quoted limits for classical deuterium isotope effects and may suggest quantum mechanical tunneling (*80*). The possible existence of tunneling has received little consideration in P450 reactions to date. Chandrasena et al. (*81*) presented Arrhenius plots for some P450 2B1 reactions over the range of 10−40 °C and did not find evidence for tunneling for *trans*-2-(*p*-trifluoromethylphenyl)cyclopropylmethane oxidation. However, more rigorous examinations using ^2H,^3H-labeled carbon substrates have not been done, to our knowledge. The high isotope effects suggest that these might be useful experiments, although the technical complexity of preparing the appropriate substrates is challenging (*82*).

In summary, we have evaluated the kinetic mechanism of rabbit P450 1A2 reactions using direct kinetic measurements of some steps and the interpretation of kinetic deuterium isotope effects. A growing body of isotope effect evidence indicates that the rate of C−H bond breaking is at least partially rate-limiting in many mammalian P450 reactions, including those catalyzed by human P450s 2D6 (*18*), 1A2 (*40*), 3A4 (*83*), 2E1 (*17*), and 2A6 (*84*). Significant noncompetitive intermolecular kinetic deuterium isotope effects have also been found in rat and hamster microsomes (*20*, *26*, *29*). With regard to the P450 1A2-specific substrate 7-methoxyresorufin, we also observed an isotope effect in rat liver microsomes, $^D(V/K) = 3.2$ (vide infra). These results, along with some of the reports of in vivo deuterium isotope effects on metabolism (*23*−*25*), suggest that C−H bond breaking is a fairly common rate-limiting step, even in microsomal and in vivo situations where reduction conditions may not be optimal. A less direct conclusion of our work is that unproductive binding modes are a general problem in the restriction of rates of catalysis, exemplified in part by some of the analyses of isotope effects (e.g., Scheme 2D, Figure 6). Further analyses of individual P450s and examination of more details of individual steps are in order.

ACKNOWLEDGMENT

We thank M. V. Martin for preparation of P450 1A2 and NADPH−P450 reductase, J. L. Sorrells for synthesis of 7-methoxyresorufin, and G. P. Miller for some of the initial experiments with deuterated 4-nitroanisole (*50*).

SUPPORTING INFORMATION AVAILABLE

Sample DynaFit files for running kinetic fits and examples of results and v vs S plots for noncompetitive intermolecular kinetic hydrogen isotope effect studies (Table 3). This material is available free of charge via the Internet at http://pubs.acs.org.

REFERENCES

1. Palmer, G., and Reedijk, J. (1992) Nomenclature of electron-transfer proteins. Recommendations 1989, *J. Biol. Chem. 267*, 665−677.
2. Northrop, D. B. (1975) Steady-state analysis of kinetic isotope effects in enzymic reactions, *Biochemistry 14*, 2644−2651.
3. Northrop, D. B. (1982) Deuterium and tritium kinetic isotope effects on initial rates, *Methods Enzymol. 87*, 607−625.
4. Ortiz de Montellano, P. R. (1995) *Cytochrome P450: Structure, Mechanism, and Biochemistry*, 2nd ed., Plenum Press, New York.
5. Guengerich, F. P. (2003) Cytochrome P450s, drugs, and diseases, *Mol. Intervent. 3*, 8−18.
6. Ortiz de Montellano, P. R., and De Voss, J. J. (2002) Oxidizing species in the mechanism of cytochrome P450, *Nat. Prod. Rep. 19*, 477−493.
7. Ortiz de Montellano, P. R. (1995) Oxygen activation and reactivity, in *Cytochrome P450: Structure, Mechanism, and Biochemistry* (Ortiz de Montellano, P. R., Ed.) 2nd ed., pp 245−303, Plenum Press, New York.
8. Guengerich, F. P. (2001) Common and uncommon cytochrome P450 reactions related to metabolism and chemical toxicity, *Chem. Res. Toxicol. 14*, 611−650.
9. White, R. E., and Coon, M. J. (1980) Oxygen activation by cytochrome P-450, *Annu. Rev. Biochem. 49*, 315−356.
10. Guengerich, F. P. (2002) Rate-limiting steps in cytochrome P450 catalysis, *Biol. Chem. 383*, 1553−1564.
11. Guengerich, F. P., Bell, L. C., and Okazaki, O. (1995) Interpretations of cytochrome P450 mechanisms from kinetic studies, *Biochimie 77*, 573−580.
12. Gigon, P. L., Gram, T. E., and Gillette, J. R. (1969) Studies on the rate of reduction of hepatic microsomal cytochrome P-450 by reduced nicotinamide adenine dinucleotide phosphate: effect of drug substrates, *Mol. Pharmacol. 5*, 109−122.
13. Diehl, H., Schädelin, J., and Ullrich, V. (1970) Studies on the kinetics of cytochrome P-450 reduction in rat liver microsomes, *Hoppe-Seyler's Z. Physiol. Chem. 351*, 1359−1371.
14. Peterson, J. A., Ebel, R. E., O'Keeffe, D. H., Matsubara, T., and Estabrook, R. W. (1976) Temperature dependence of cytochrome

P-450 reduction: a model for NADPH-cytochrome P-450 reductase: cytochrome P-450 interaction, *J. Biol. Chem. 251*, 4010−4016.
15. Björkhem, I. (1982) Rate-limiting step in microsomal cytochrome P-450 catalyzed hydroxylations, in *Hepatic Cytochrome P-450 Monooxygenase System* (Schenkman, J. B., and Kupfer, D., Eds.) pp 645−666, Pergamon Press, New York.
16. Gander, J. E., and Mannering, G. J. (1982) Kinetics of hepatic cytochrome P-450-dependent mono-oxygenase systems, in *Hepatic Cytochrome P-450 Monooxygenase System* (Schenkman, J. B., and Kupfer, D., Eds.) pp 667−697, Pergamon Press, New York.
17. Bell-Parikh, L. C., and Guengerich, F. P. (1999) Kinetics of cytochrome P450 2E1-catalyzed oxidation of ethanol to acetic acid via acetaldehyde, *J. Biol. Chem. 274*, 23833−23840.
18. Guengerich, F. P., Miller, G. P., Hanna, I. H., Sato, H., and Martin, M. V. (2002) Oxidation of methoxyphenethylamines by cytochrome P450 2D6. Analysis of rate-limiting steps, *J. Biol. Chem. 277*, 33711−33719.
19. Johnson, K. A. (2003) Introduction to kinetic analysis of enzyme systems, in *Kinetic Analysis of Macromolecules. A Practical Approach* (Johnson, K. A., Ed.) pp 1−18, Oxford University Press, Oxford, U.K.
20. Foster, A. B., Jarman, M., Stevens, J. D., Thomas, P., and Westwood, J. H. (1974) Isotope effects in *O*- and *N*-demethylations mediated by rat liver microsomes: an application of direct insertion electron impact mass spectrometry, *Chem-Biol. Interact. 9*, 327−340.
21. Hjelmeland, L. M., Aronow, L., and Trudell, J. R. (1977) Intramolecular determination of primary kinetic isotope effects in hydroxylations catalyzed by cytochrome P-450, *Biochem. Biophys. Res. Commun. 76*, 541−549.
22. Groves, J. T., McClusky, G. A., White, R. E., and Coon, M. J. (1978) Aliphatic hydroxylation by highly purified liver microsomal cytochrome P-450: Evidence for a carbon radical intermediate, *Biochem. Biophys. Res. Commun. 81*, 154−160.
23. Keefer, L. K., Lijinsky, W., and Garcia, H. (1973) Deuterium isotope effect on the carcinogenicity of dimethylnitrosamine in rat liver, *J. Natl. Cancer Inst. 51*, 299−302.
24. Funaki, T., Soons, P. A., Guengerich, F. P., and Breimer, D. D. (1989) In vivo oxidative cleavage of a pyridine carboxylic acid ester of nifedipine, *Biochem. Pharmacol. 38*, 4213−4216.
25. Jarman, M., Poon, G. K., Rowlands, M. G., Grimshaw, R. M., Horton, M. N., Potter, G. A., and McCague, R. (1995) The deuterium isotope efffect for the α-hydroxylation of tamoxifen by rat liver microsomes accounts for the reduced genotoxicity of [D_5-ethyl]tamoxifen, *Carcinogenesis 16*, 683−688.
26. Miwa, G. T., and Lu, A. Y. H. (1987) Kinetic isotope effects and 'metabolic switching' in cytochrome P450-catalyzed reactions, *BioEssays 7*, 215−219.
27. Miwa, G. T., Walsh, J. S., and Lu, A. Y. H. (1984) Kinetic isotope effects on cytochrome P-450-catalyzed oxidation reactions: the oxidative O-dealkylation of 7-ethoxycoumarin, *J. Biol. Chem. 259*, 3000−3004.
28. Harada, N., Miwa, G. T., Walsh, J. S., and Lu, A. Y. H. (1984) Kinetic isotope effects on cytochrome P-450-catalyzed oxidation reactions: evidence for the irreversible formation of an activated oxygen intermediate of cytochrome P-448, *J. Biol. Chem. 259*, 3005−3010.
29. Miwa, G. T., Harada, N., and Lu, A. Y. H. (1985) Kinetic isotope effects on cytochrome P-450-catalyzed oxidation reactions: full expression of the intrinsic isotope effect during the O-deethylation of 7-ethoxycoumarin by liver microsomes from 3-methylcholanthrene-induced hamsters, *Arch. Biochem. Biophys. 239*, 155−162.
30. Jones, J. P., Korzekwa, K. R., Rettie, A. E., and Trager, W. F. (1986) Isotopically sensitive branching and its effect on the observed intramolecular isotope effects in cytochrome P-450 catalyzed reactions: a new method for the estimation of intrinsic isotope effects, *J. Am. Chem. Soc. 108*, 7074−7078.
31. Jones, J. P., and Trager, W. F. (1987) The separation of the intramolecular isotope effect for the cytochrome P-450 catalyzed hydroxylation of *n*-octane into its primary and secondary components, *J. Am. Chem. Soc. 109*, 2171−2173.
32. Korzekwa, K. R., Trager, W. F., and Gillette, J. R. (1989) Theory for the observed isotope effects from enzymatic systems that form multiple products via branched reaction pathways: cytochrome P-450, *Biochemistry 28*, 9012−9018.
33. Korzekwa, K. R., Jones, J. P., and Gillette, J. R. (1990) Theoretical studies on cytochrome P-450 mediated hydroxylation: a predictive model for hydrogen atom abstractions, *J. Am. Chem. Soc. 112*, 7042−7046.
34. Gillette, J. R., Darbyshire, J. F., and Sugiyama, K. (1994) Theory for the observed isotope effects on the formation of multiple products by different kinetic mechanisms of cytochrome P450 enzymes, *Biochemistry 33*, 2927−2937.
35. Gelb, M. H., Heimbrook, D. C., Mälkönen, P., and Sligar, S. G. (1982) Stereochemistry and deuterium isotope effects in camphor hydroxylation by the cytochrome $P450_{cam}$ monoxygenase system, *Biochemistry 21*, 370−377.
36. Atkins, W. M., and Sligar, S. G. (1987) Metabolic switching in cytochrome $P\text{-}450_{cam}$: deuterium isotope effects on regiospecificity and the monooxygenase/oxidase ratio, *J. Am. Chem. Soc. 109*, 3754−3760.
37. Kadkhodayan, S., Coulter, E. D., Maryniak, D. M., Bryson, T. A., and Dawson, J. H. (1995) Uncoupling oxygen transfer and electron transfer in the oxygenation of camphor analogues by cytochrome P450-CAM: direct observation of an *inter*molecular isotope effect for substrate C−H activation, *J. Biol. Chem. 270*, 28042−28048.
38. Guengerich, F. P., Peterson, L. A., and Böcker, R. H. (1988) Cytochrome P-450-catalyzed hydroxylation and carboxylic acid ester cleavage of Hantzsch pyridine esters, *J. Biol. Chem. 263*, 8176−8183.
39. Bell, L. C., and Guengerich, F. P. (1997) Oxidation kinetics of ethanol by human cytochrome P450 2E1. Rate-limiting product release accounts for effects of isotopic hydrogen substitution and cytochrome b_5 on steady-state kinetics, *J. Biol. Chem. 272*, 29643−29651.
40. Yun, C.-H., Miller, G. P., and Guengerich, F. P. (2000) Rate-determining steps in phenacetin oxidations by human cytochrome P450 1A2 and selected mutants, *Biochemistry 39*, 11319−11329.
41. Yun, C.-H., Miller, G. P., and Guengerich, F. P. (2001) Oxidations of *p*-alkoxyacylanilides by human cytochrome P450 1A2: structure−activity relationships and simulation of rate constants of individual steps in catalysis, *Biochemistry 40*, 4521−4530.
42. Graham-Lorence, S., Truan, G., Peterson, J. A., Falck, J. R., Wei, S., Helvig, C., and Capdevila, J. H. (1997) An active site substitution, F87V, converts cytochrome P450 BM-3 into a regio- and stereoselective (14*S*,15*R*)-arachidonic acid epoxygenase, *J. Biol. Chem. 272*, 1127−1135.
43. Parikh, A., Josephy, P. D., and Guengerich, F. P. (1999) Selection and characterization of human cytochrome P450 1A2 mutants with altered catalytic properties, *Biochemistry 38*, 5283−5289.
44. Guengerich, F. P. (2002) Cytochrome P450 enzymes in the generation of commercial products, *Nat. Rev., Drug Discov. 1*, 359−366.
45. Sandhu, P., Guo, Z., Baba, T., Martin, M. V., Tukey, R. H., and Guengerich, F. P. (1994) Expression of modified human cytochrome P450 1A2 in *Escherichia coli*: stabilization, purification, spectral characterization, and catalytic activities of the enzyme, *Arch. Biochem. Biophys. 309*, 168−177.
46. Haugen, D. A., and Coon, M. J. (1976) Properties of electrophoretically homogenous phenobarbital-inducible and β-naphthoflavone-inducible forms of liver microsomal cytochrome P-450, *J. Biol. Chem. 251*, 7929−7939.
47. Oprian, D. D., Vatsis, K. P., and Coon, M. J. (1979) Kinetics of reduction of cytochrome $P\text{-}450LM_4$ in a reconstituted liver microsomal enzyme system, *J. Biol. Chem. 254*, 8895−8902.
48. Oprian, D. D., and Coon, M. J. (1980) Formation and decay of oxygenated $P\text{-}450_{LM4}$, in *Biochemistry, Biophysics and Regulation of Cytochrome P-450* (Gustafsson, J.-Å., Carlstedt-Duke, J., Mode, A., and Rafter, J., Eds.) pp 323−330, Elsevier/North-Holland Biomedical Press, Amsterdam.
49. Backes, W. L., Batie, C. J., and Cawley, G. F. (1998) Interactions among P450 enzymes when combined in reconstituted systems: formation of a 2B4−1A2 complex with a high affinity for NADPH-cytochrome P450 reductase, *Biochemistry 37*, 12852−12859.
50. Miller, G. P., and Guengerich, F. P. (2001) Binding and oxidation of alkyl 4-nitrophenyl ethers by rabbit cytochrome P450 1A2: evidence for two binding sites, *Biochemistry 40*, 7262−7272.
51. Ruzicka, E., and Jurina, J. (1966) Resazurin ethers, *Monatsh. Chem. 97*, 129−134.
52. Alterman, M. A., and Dowgii, A. I. (1990) A simple and rapid method for the purification of cytochrome P-450 (form LM4), *Biomed. Chromatogr. 4*, 221−222.

53. Guengerich, F. P., Dannan, G. A., Wright, S. T., Martin, M. V., and Kaminsky, L. S. (1982) Purification and characterization of liver microsomal cytochromes P-450: electrophoretic, spectral, catalytic, and immunochemical properties and inducibility of eight isozymes isolated from rats treated with phenobarbital or β-naphthoflavone, *Biochemistry 21*, 6019−6030.
54. Hanna, I. H., Teiber, J. F., Kokones, K. L., and Hollenberg, P. F. (1998) Role of the alanine at position 363 of cytochrome P450 2B2 in influencing the NADPH- and hydroperoxide-supported activities, *Arch. Biochem. Biophys. 350*, 324−332.
55. Guengerich, F. P. (2001) Analysis and characterization of enzymes and nucleic acids, in *Principles and Methods of Toxicology* (Hayes, A. W., Ed.) 4th ed., pp 1625−1687, Taylor & Francis, New York.
56. Josephy, P. D., and Van Damme, A. (1984) Reaction of Gibbs reagent with *para*-substituted phenols, *Anal. Chem. 56*, 813−814.
57. Gorsky, L. D., Koop, D. R., and Coon, M. J. (1984) On the stoichiometry of the oxidase and monooxygenase reactions catalyzed by liver microsomal cytochrome P-450: products of oxygen reduction, *J. Biol. Chem. 259*, 6812−6817.
58. Guengerich, F. P., Yun, C.-H., and Macdonald, T. L. (1996) Evidence for a one-electron oxidation mechanism in N-dealkylation of *N*,*N*-dialkylanilines by cytochrome P450 2B1. Kinetic hydrogen isotope effects, linear free energy relationships, comparisons with horseradish peroxidase, and studies with oxygen surrogates, *J. Biol. Chem. 271*, 27321−27329.
59. Okazaki, O., and Guengerich, F. P. (1993) Evidence for specific base catalysis in *N*-dealkylation reactions catalyzed by cytochrome P450 and chloroperoxidase: differences in rates of deprotonation of aminium radicals as an explanation for high kinetic hydrogen isotope effects observed with peroxidases, *J. Biol. Chem. 268*, 1546−1552.
60. Burleigh, B. D., Jr., Foust, G. P., and Williams, C. H., Jr. (1969) A method for titrating oxygen-sensitive organic redox systems with reducing agents in solution, *Anal. Biochem. 27*, 536−544.
61. Guengerich, F. P. (1983) Oxidation−reduction properties of rat liver cytochrome P-450 and NADPH-cytochrome P-450 reductase related to catalysis in reconstituted systems, *Biochemistry 22*, 2811−2820.
62. Kuzmic, P. (1996) Program DYNAFIT for the analysis of enzyme kinetic data: application to HIV protease, *Anal. Biochem. 237*, 260−273.
63. Patel, S. S., Bandwar, R. P., and Levin, M. K. (2003) Transient-state kinetics and computational analysis of transcription initiation, in *Kinetic Analysis of Macromolecules. A Practical Approach* (Johnson, K. A., Ed.) pp 87−129, Oxford University Press, Oxford, U.K.
64. Walsh, C. (1979) *Enzymatic Reaction Mechanisms*, W. H. Freeman Co., San Francisco.
65. Estabrook, R. W., Franklin, M. R., Cohen, B., Shigamatzu, A., and Hildebrandt, A. G. (1971) Biochemical and genetic factors influencing drug metabolism. Influence of hepatic microsomal mixed function oxidation reactions on cellular metabolic control, *Metabolism 20*, 187−199.
66. Weaver, R. J., Thompson, S., Smith, G., Dickins, M., Elcombe, C. R., Mayer, R. T., and Burke, M. D. (1994) A comparative study of constitutive and induced alkoxyresorufin O-dealkylation and individual cytochrome P450 forms in cynomolgus monkey (*Macaca fascicularis*), human, mouse, rat and hamster liver microsomes, *Biochem. Pharmacol. 47*, 763−773.
67. Burke, M. D., Thompson, S., Weaver, R. J., Wolf, C. R., and Mayer, R. T. (1994) Cytochrome P450 specificities of alkoxyresorufin O-dealkylation in human and rat liver, *Biochem. Pharmacol. 48*, 923−936.
68. Guengerich, F. P., and Johnson, W. W. (1997) Kinetics of ferric cytochrome P450 reduction by NADPH-cytochrome P450 reductase: Rapid reduction in absence of substrate and variations among cytochrome P450 systems, *Biochemistry 36*, 14741−14750.
69. Oprian, D. D., Gorsky, L. D., and Coon, M. J. (1983) Properties of the oxygenated form of liver microsomal cytochrome P-450, *J. Biol. Chem. 258*, 8684−8691.
70. Tyson, C. A., Lipscomb, J. D., and Gunsalus, I. C. (1972) The roles of putidaredoxin and P450cam in methylene hydroxylation, *J. Biol. Chem. 247*, 5777−5784.
71. Schlichting, I., Berendzen, J., Chu, K., Stock, A. M., Maves, S. A., Benson, D. E., Sweet, B. M., Ringe, D., Petsko, G. A., and Sligar, S. G. (2000) The catalytic pathway of cytochrome P450cam at atomic resolution, *Science 287*, 1615−1622.
72. Hosea, N. A., Miller, G. P., and Guengerich, F. P. (2000) Elucidation of distinct binding sites for cytochrome P450 3A4, *Biochemistry 39*, 5929−5939.
73. Lichtenberger, F., Nastainczyk, W., and Ullrich, V. (1976) Cytochrome P-450 as an oxene transferase, *Biochem. Biophys. Res. Commun. 70*, 939−946.
74. Burka, L. T., Thorsen, A., and Guengerich, F. P. (1980) Enzymatic monooxygenation of halogen atoms: cytochrome P-450 catalyzed oxidation of iodobenzene by iodosobenzene, *J. Am. Chem. Soc. 102*, 7615−7616.
75. Mansuy, D., Bartoli, J. F., and Momenteau, M. (1982) Alkane hydroxylation catalyzed by metalloporphyrins: evidence for different active oxygen species with alkylhydroperoxides and iodosobenzene as oxidants, *Tetrahedron Lett. 23*, 2781−2784.
76. Ortiz de Montellano, P. R. (1986) Oxygen activation and transfer, in *Cytochrome P-450* (Ortiz de Montellano, P. R., Ed.) 1st ed., pp 217−271, Plenum Press, New York.
77. Hanna, I. H., Krauser, J. A., Cai, H., Kim, M.-S., and Guengerich, F. P. (2001) Diversity in mechanisms of substrate oxidation by cytochrome P450 2D6. Lack of an allosteric role of NADPH-cytochrome P450 reductase in catalytic regioselectivity, *J. Biol. Chem. 276*, 39553−39561.
78. White, R. E., Miller, J. P., Favreau, L. V., and Bhattacharyya, A. (1986) Stereochemical dynamics of aliphatic hydroxylation by cytochrome P-450, *J. Am. Chem. Soc. 108*, 6024−6031.
79. Mueller, E. J., Loida, P. J., and Sligar, S. G. (1995) Twenty-five years of $P450_{cam}$ research: mechanistic insights into oxygenase catalysis, in *Cytochrome P450: Structure, Mechanism, and Biochemistry* (Ortiz de Montellano, P. R., Ed.) 1st ed., pp 83−124, Plenum Press, New York.
80. Cha, Y., Murray, C. J., and Klinman, J. P. (1989) Hydrogen tunneling in enzyme reactions, *Science 243*, 1325−1330.
81. Chandrasena, R. E., Vatsis, K. P., Coon, M. J., Hollenberg, P. F., and Newcomb, M. (2004) Hydroxylation by the hydroperoxy-iron species in cytochrome P450 enzymes, *J. Am. Chem. Soc. 126*, 115−126.
82. Knapp, M. J., and Klinman, J. P. (2002) Environmentally coupled hydrogen tunneling. Linking catalysis to dynamics, *Eur. J. Biochem. 269*, 3113−3121.
83. Krauser, J. A., and Guengerich, F. P. (2003) Investigation of C−H bond cleavage by cytochrome P450 3A4, in *Abstracts*, *226th National Meeting of the American Chemical Society*, Sept 7−11, TOXI 80, New York.
84. Calcutt, W., and Guengerich, F. P. (2003) Kinetic isotope effects in dialkylnitrosamine dealkylations catalyzed by human cytochrome P450s 2A6 and 2E1, *FASEB J. 17*, A1325.

BI0491393